This is a repository copy of *CD9 co-operation with syndecan-1 is required for a major staphylococcal adhesion pathway*.

White Rose Research Online URL for this paper:
https://eprints.whiterose.ac.uk/201941/

Version: Published Version

Article:

🔓 | Host-Microbial Interactions | Research Article

CD9 co-operation with syndecan-1 is required for a major staphylococcal adhesion pathway

Luke R. Green,[1] Rahaf Issa,[1] Fawzyah Albaldi,[2] Lucy Urwin,[1] Ruth Thompson,[3] Henna Khalid,[2] Claire E. Turner,[2] Barbara Ciani,[4] Lynda J. Partridge,[2] Peter N. Monk[1]

AUTHOR AFFILIATIONS See affiliation list on p. 19.

ABSTRACT Epithelial colonization is a critical first step in bacterial pathogenesis. *Staphylococcus aureus* can utilize several host factors to associate with cells, including α5β1 integrin and heparan sulfate proteoglycans, such as the syndecans. Here, we demonstrate that a partner protein of both integrins and syndecans, the host membrane adapter protein tetraspanin CD9, is essential for syndecan-mediated staphylococcal adhesion. Fibronectin is also essential in this process, while integrins are only critical for post-adhesion entry into human epithelial cells. Treatment of epithelial cells with CD9-derived peptide or heparin caused significant reductions in staphylococcal adherence, dependent on both CD9 and syndecan-1. Exogenous fibronectin caused a CD9-dependent increase in staphylococcal adhesion, whereas blockade of β1 integrins did not affect adhesion but did reduce the subsequent internalization of adhered bacteria. CD9 disruption or deletion increased β1 integrin-mediated internalization, suggesting that CD9 coordinates sequential staphylococcal adhesion and internalization. CD9 controls staphylococcal adhesion through syndecan-1, using a mechanism that likely requires CD9-mediated syndecan organization to correctly display fibronectin at the host cell surface. We propose that CD9-derived peptides or heparin analogs could be developed as anti-adhesion treatments to inhibit the initial stages of staphylococcal pathogenesis.

IMPORTANCE *Staphylococcus aureus* infection is a significant cause of disease and morbidity. *Staphylococci* utilize multiple adhesion pathways to associate with epithelial cells, including interactions with proteoglycans or β1 integrins through a fibronectin bridge. Interference with another host protein, tetraspanin CD9, halves staphylococcal adherence to epithelial cells, although CD9 does not interact directly with bacteria. Here, we define the role of CD9 in staphylococcal adherence and uptake, observing that CD9 coordinates syndecan-1, fibronectin, and β1 integrins to allow efficient staphylococcal infection. Two treatments that disrupt this action are effective and may provide an alternative to antibiotics. We provide insights into the mechanisms that underlie staphylococcal infection of host cells, linking two known adhesion pathways together through CD9 for the first time.

KEYWORDS CD9, HSPG, *Staphylococcus aureus*, bacterial adhesion, fibronectin, epithelial, syndecan, tetraspanin

S*taphylococcus aureus* is an opportunistic pathogen and a common causative agent of community and nosocomial infections. Infections result in a myriad of clinical outcomes ranging from superficial skin infections to systemic infections, including pneumonia, endocarditis, and osteomyelitis (1). Furthermore, the rapid acquisition of various antimicrobial resistance mechanisms by *S. aureus* worldwide (2) makes the study of this organism, and development of potential therapeutics, critical for healthcare. *S.*

aureus has adapted a range of adhesins for adherence to host cell surface molecules, allowing for efficient downstream entry into cells (3). Several of these adhesins bind to the extracellular matrix (ECM) protein, fibronectin (Fn). The canonical cellular staphylococcal adhesion and internalization pathway utilize Fn-binding proteins (FnBPs) to bind to Fn using a zipper-like mechanism (4). On the host cell surface, Fn binds to α5β1 integrins through an RGD motif, leading to the proposal that Fn acts as a bridge between the host and the pathogen. The FnBP-Fn-α5β1 complex is thought to be central to *S. aureus* adhesion and internalization (3).

S. aureus can also utilize heparan sulfate proteoglycans (HSPGs), such as the syndecans (SDC), to adhere and gain entry into host cells (5). Many bacteria utilize the glycosaminoglycan (GAG) heparan sulfate (HS) moiety of proteoglycans (PG), using these negatively charged polysaccharides as binding sites for clusters of positively charged amino acids within FnBPs (6). SDC-1 in particular has been associated with *S. aureus* adherence to intestinal, lung, and corneal epithelial cell lines, since interactions were blocked using HS mimics such as heparin (5, 7, 8). SDC-1$^{-/-}$ mice were also more resistant to corneal infection by *S. aureus*; however, no specific binding of *S. aureus* to SDC-1 was demonstrated, suggesting that it is not directly involved in attachment (9). SDC can also bind Fn through HepII domains (10) and has been shown to modulate Fn fibrillogenesis in an integrin-dependent manner (11). This has led to suggestions that SDC, integrins, and Fn collaborate in the formation of binding sites on host cells that are exploited by many pathogenic bacteria, for example, *Streptococcus pneumoniae* (12). However, the molecular details of these interactions are currently unknown.

The tetraspanins are a superfamily of transmembrane proteins whose major function is to organize various proteins at the cell surface into dynamic structured "islands," known as tetraspanin-enriched microdomains (TEMs) (13). There are 33 human tetraspanins with conserved structural motifs, four transmembrane domains, a small (EC1) and large (EC2) extracellular loop, and generally short N- and C-terminal domains. The crystal structures of CD9 and CD81 demonstrate a reverse cone-like structure creating a lipid binding pocket within the transmembrane domains. Lipid interactions with this pocket are thought to change the conformation of the tetraspanin between an "open" and "closed" state (14, 15). In the open state, the EC2 domain is available for partner protein interactions that mediate the involvement of TEMs in a wide variety of cellular functions (16). For example, the tetraspanins have been shown to organize partner proteins into "adhesive platforms" to allow leukocyte adhesion to endothelial cells (17). Partner proteins can include integrins, HSPGs, and immunoglobulin superfamily members (14), many of which are important in host cell adherence and entry of microbial pathogens. The tetraspanins have been implicated in a number of different viral and bacterial infections (18, 19). We have previously demonstrated that tetraspanin blockade, using antibodies or recombinant EC2 domains, can significantly reduce Gram-negative and Gram-positive bacterial adherence to epithelial cells (20). We further showed that short CD9 EC2-derived peptides were able to significantly reduce *S. aureus* adherence to keratinocytes and to an engineered model of human skin (21). While tetraspanins can act as receptors for other bacteria, for example, *Mycobacterium abscessus* (22, 23), our studies demonstrate that in this instance, CD9 acts as a mediator of bacterial adherence and not as a direct receptor (20).

In the present study, we demonstrate for the first time that the tetraspanin, CD9, is a critical component of an SDC-1/Fn adhesion network exploited by *S. aureus* as a primary means of adhesion to human epithelial cells. Staphylococcal adherence was significantly reduced by both a CD9 EC2-derived peptide and soluble GAG analogs (heparins), but no additive effect was observed in combination. We show that proteoglycan SDC-1 is essential for these inhibitory effects. Addition of exogenous Fn to epithelial cells increased staphylococcal adherence, but this was completely abrogated by CD9 EC2-derived peptide. Integrin α5β1 blockade had no effect on bacterial adherence, but CD9 appeared to inhibit α5β1-mediated staphylococcal internalization, suggesting that CD9 coordinates adhesion and internalization. Taken together, our study demonstrates

the critical importance of CD9 during Fn-mediated staphylococcal adherence and highlights the potential of the tetraspanin-derived peptides and heparins as anti-adhesive therapeutics for bacterial infections.

MATERIALS AND METHODS

Strains and bacterial growth conditions

S. aureus strains, SH1000 and SH1000 Δ*fnb*, were kindly provided by Simon Foster (University of Sheffield, Sheffield, United Kingdom). MRSA isolates were retrieved from skin infections of patients at Northern General Hospital, Sheffield, and kindly provided by Sue Whittaker. Liquid cultures were grown in Luria broth (LB; Oxoid, Ltd., Basingstoke, United Kingdom) microaerobically at 37°C in a humidified atmosphere with constant agitation. OD_{600nm} readings were taken using a Varioskan LUX microplate reader (ThermoFisher Scientific, Waltham, MA, USA). Solid cultures were grown on LB agar (Oxoid) overnight at 37°C. Freshly grown plates were used to inoculate all liquid cultures.

Cell culture

Wild-type (WT) and CD9 knockout ($^{-/-}$) A549 human lung epithelial cells were a gift from David Blake (Fort Lewis College, CO, USA) (24), while Tspan15$^{-/-}$ A549 cells were obtained from Mike Tomlinson (University of Birmingham, Birmingham, United Kingdom). HaCaT cells, a human keratinocyte cell line, were supplied by Cell Lines Service (CLS GmbH, Eppelheim, Germany). IPEC-J2 cells, a porcine intestinal epithelial cell line, were supplied by DSMZ-German Collection of Microorganisms and Cell Culture (Braunschweig, Germany). The above cell lines were maintained in Dulbecco's Modified Eagle's Media (DMEM; ThermoFisher Scientific) and 10% heat-inactivated fetal calf serum (FCS; Labtech International Ltd., Heathfield, United Kingdom). HCE-2 (ATCC, Manassas, VA, USA), a human corneal epithelial cell line, was cultured in keratinocyte serum-free media (KSFM; ThermoFisher Scientific) supplemented with hydrocortisone, insulin, epidermal growth factor, and bovine pituitary extract.

Primary normal human tonsillar keratinocytes (NTKs) were a gift from Craig Murdoch and Helen Colley (School of Clinical Dentistry, University of Sheffield, United Kingdom). NTKs were isolated from palatine tonsils collected from patients during routine tonsillectomies at the Royal Hallamshire Hospital, Sheffield Teaching Hospitals NHS Foundation Trust, with written, informed consent (UK National Research Ethical Committee approval number 09 /H1308/66) and cultured in a flavin- and adenine-enriched medium as previously described (25). For experiments, cells were differentially trypsinized to remove the irradiated 3T3 fibroblast feeder layer, and NTKs were seeded on surfaces coated with 100 µg/mL type IV human collagen (Merck) in defined keratinocyte serum-free medium (ThermoFisher Scientific) supplemented with Y-27632 (Abcam plc, Cambridge, United Kingdom).

Peptides, antibodies, and GAGs

Peptides were synthesized using solid phase Fmoc chemistry (Genscript, Piscataway, NJ, USA). The CD9 EC2-derived peptide, 800C (DEPQRETLKAIHYALN), was designed using the 15 residue segment of the second α-helix from the EC2 domain, previously demonstrated to inhibit staphylococcal interactions with human cells (21). A homologous EC2-derived peptide was designed from the related tetraspanin CD81 (CD81 P1: DANNAKAVVKTFHETLD). Scrambled peptides were randomly generated from the CD9 (QEALKYNRAEETPLDIH) and CD81 sequences (ADTDALVNKFTKHANEV). Fluorescently labeled peptides were synthesized with a 6-carboxyfluorescein moiety at the N-terminus. Integrin RGD peptides (GRGDS and SDGRG), heparinase I/III, chondroitinase ABC, and fondaparinux were obtained from Merck KGaA, Darmstadt, Germany. Unfractionated heparin (UFH) (LEO Pharma A/S, Ballerup, Denmark) and dalteparin were obtained from the Royal Hallamshire Hospital Pharmacy, United Kingdom. Heparan sulfate, chondroitin

sulfate (CS), and dermatan sulfate (DS) were supplied by Iduron, Macclesfield, Unite Kingdom. Mouse anti-human CD9 IgG1 (MM2/57; Merck), mouse anti-human SDC-1 IgG1 (B-A38; Santa Cruz Biotechnology, Dallas, TX, USA), mouse anti-human SDC-4 IgG2a (5G9; Santa Cruz Biotechnology), rat anti-human β1 IgG1 (AIIB2; Merck), mouse anti-human β1 IgG1 (Lia1/2; GeneTex, Irvine, CA, USA), mouse anti-human α5 IgG_1 (JBS5; Merck), mouse anti-human α5 IgG3 (P1D6; Merck), mouse anti-FLAG (M2; Merck), mouse IgG1 (JC1; in house), mouse IgG2a (02–6200; Thermofisher Scientific), mouse IgG3 (B10; Thermofisher Scientific) and rat IgG1 (14–4301-82; Thermofisher Scientific), mouse IgG1 ascites fluid (MOPC 21; Merck), and goat anti-mouse HRP (P0447; Agilent, Santa Clara, CA, USA) were used as described. Pixatimod was kindly provided by Zucero Pty, Brisbane, Australia.

SDC knockdown by shRNA

Short hairpin RNA (shRNA) targeting SDC-1 and SDC-4 or a nonsense control inserted into the lentiviral plasmid pLVTHM were obtained from Andreas Ludwig (RWTH Aachen University, Germany) (26, 27). Sub-confluent HEK293T cells were co-transfected with 2.6 µg pMD2G (Addgene, Watertown, MA, USA), 7.4 µg psPAX2 (Addgene), and 10 µg pLVTHM with 10 µL jetPEI (Polyplus transfection, Illkirch-Graffenstaden, France) to produce recombinant lentiviruses. After 24 h, media were changed and the resulting lentivirus-containing supernatants were harvested after a further 48 h. For transient transfection, 2×10^5 WT cells were grown for 24 h before replacement of 20% of the culture media with lentivirus-containing supernatant. Transduction efficiency was enhanced through addition of polybrene (Merck). GFP expression was used to assess the efficiency of transduction, and flow cytometry was used to measure the expression of SDC-1 and SDC-4.

Expression analysis

Tetraspanin and staphylococcal receptor expression was measured by flow cytometry. 1×10^6 adherent cells were detached using cell dissociation buffer (ThermoFisher Scientific) and labeled with the relevant antibody at 4°C for 60 min. A fluorescein isothiocyanate (FITC) conjugated goat anti-mouse IgG antibody (F5387, Merck) was used for secondary labeling if required. Cells were fixed with 1% paraformaldehyde, analyzed with an LSRII cytometer (Becton Dickinson, Oxford, United Kingdom) using FlowJo v10.0.7r2 software (BD).

Fluorescent 800C binding

WT or $CD9^{-/-}$ cells were seeded at 2.5×10^5 onto sterile 22 mm glass coverslips and incubated overnight at 37°C with 8% CO_2. Cells were washed with PBS, before addition of 200 nM 6-carboxyfluorescein (FAM) tagged peptide or media alone for 30 min at 37°C. Cells were fixed with 2% PFA for 15 min before being washed twice. Coverslips were placed on slides with Vectashield Mounting Media with DAPI (Maravai LifeSciences, San Diego, CA, USA) and imaged using a Nikon Ti Eclipse microscope. Images were analyzed using ImageJ, and corrected total fluorescence intensity was calculated as follows: total cell fluorescence = integrated density − (area of selected cell or whole image × mean fluorescence of background).

Infection assays

Cells (2×10^4)were seeded onto 96 well plates and cultured overnight. Five percent bovine serum albumin (BSA; Merck) was added to cells for 60 min to reduce non-specific binding. Cells were washed with PBS and treated with peptide, antibodies, or blocking reagents for a further 60 min. Cells were infected at a multiplicity of infection (MOI) of 50 for 60 min at 37°C with 5% CO_2. Cells were washed four times with PBS and lysed with 2% saponin (Merck) for 30 min. Lysates were serially diluted, plated onto LB agar plates, and allowed to grow overnight at 37°C. To further control for non-specific plastic binding, the number of bacteria bound to BSA blocked empty wells was subtracted from

adherent and internalized bacteria. Bacterial adherence to treated cells was calculated as a percentage of bacterial adherence to untreated cells which was set at 100%.

For enumeration by microscopy, 1.5×10^5 WT cells were seeded onto glass coverslips in 24 well plates and cultured overnight. Cells were blocked, treated, and infected as described above. Cells were washed four times with PBS after infection to remove unbound bacteria. Coverslips were fixed with a methanol:acetic acid (3:1) solution for 5 min. Fixed cells were washed with distilled water and stained with 10% Giemsa stain for 20 min. Coverslips were mounted and viewed by light microscopy. A undred cells were counted from various fields of view and scored for the number of infected cells and the total number of adhered bacteria.

Gentamicin protection assays

Infection assays were carried out as described. After infection, cells were washed four times with PBS before immersion in cell media with 200 µg/mL gentamicin for 1 h to eliminate extracellular bacteria. Wells containing no cells were used to ensure efficient killing of bacteria by the antibiotic. Cells were washed twice with PBS and lysed with 2% saponin for 30 min. Lysates were serially diluted and plated onto LB agar before overnight incubation at 37°C.

Co-immunoprecipitation

Whole cell lysates were prepared in RIPA buffer (10 mM Tris-HCl pH 8.0, 1 mM EDTA, 0.5 mM EGTA, 1% Triton X-100, 0.1% sodium deoxycholate, 0.1% SDS, and 140 mM NaCl) with a protease inhibitor cocktail (Complete Mini, Roche, Basel, Switzerland). Protein-G magnetic beads (Dynabeads, ThermoFisher Scientific) were incubated with anti-CD9 antibody (4 µg) at room temperature on a rotator for 10 min. Lysates were incubated with antibody-labeled beads for 60 min at 4°C on a rotator. Beads were washed three times in PBS-Triton X-100 (0.2%), boiled in RIPA buffer, and the elute was separated by SDS-PAGE. Blots were probed with anti-CD9 or anti-SDC-1 (1:1,000) antibodies and detected with the corresponding secondary HRP-conjugated antibody. Immunoprecipitation of lysates with an anti-FLAG antibody was used as an appropriate control.

Statistical analyses

All analyses were performed within GraphPad Prism version 9.5.0 (GraphPad Software Inc., Boston, MA, USA). Significance was established at $P \leq 0.05$, all data presented represent at least three independent experiments. Statistical considerations and specific analyses are described separately within each section. * specifies significance to the untreated control unless otherwise specified; $*P \leq 0.05$, $**P \leq 0.01$, and $***P \leq 0.001$.

RESULTS

CD9-blockade reduces staphylococcal adherence to cells

Tetraspanins, HSPGs, and β1 integrins have individually been demonstrated to be involved in staphylococcal adherence and internalization (4, 5, 20, 21). To investigate the relationship between these groups of molecules, staphylococcal adherence was measured by colony forming unit (CFU) after treatment of WT A549 or tetraspanin CD9$^{-/-}$ A549 cells with a CD9-derived peptide (800C). CD9 was well expressed in WT cells but significantly reduced in CD9$^{-/-}$ cells (Fig. S1A and B). 800C significantly reduced *S. aureus* SH1000 adherence to WT cells at 20 nM (48.7 ± 11.6%) but was slightly less effective at 2 nM (29.3 ± 9.2%; Fig. 1A). Pre-treatment with a scrambled 800C sequence peptide caused no significant reduction at concentrations up to 200 nM (Fig. 1A). With untreated CD9$^{-/-}$ cells, staphylococcal adherence was significantly reduced compared to untreated WT cells (41.5 ± 11.4%; Fig. S1C) but treatment with 800C or the scrambled peptide had no further effect on staphylococcal adherence (Fig. 1A). 800C and the scrambled peptide did not inhibit staphylococcal growth at a range of concentrations (Fig. S2A

and B). Tspan15, a different tetraspanin, contains eight cysteine residues within the EC2 domain compared to the four within CD9. This leads to a significantly different structure within the EC2 and a differing set of partner proteins compared to CD9 (28). Knockout of Tspan15 also reduced staphylococcal adherence to untreated cells (24.5 ± 10.5%; Fig. S1C) but 800C was still inhibitory (49.4 ± 6.4%; Fig. S3A) suggesting that the peptide specifically acts on CD9. This was further confirmed as treatment of WT cells with a homologous peptide derived from tetraspanin CD81, which has a similar tertiary structure to CD9 but differs in amino acid sequence, had no effect (Fig. S4A and B). In addition, fluorescently tagged 800C specifically bound to WT cells at higher levels than its scrambled peptide control, while binding to CD9$^{-/-}$ cells was similar to that of the scrambled peptide (Fig. S4C through E). The inhibition of adhesion by 800C was also observed with a clinically relevant *S. aureus* strain, MRSA1 (Fig. S5A). Thus, we have identified a staphylococcal adherence pathway that can be inhibited by 800C only in the presence of CD9 on host cells.

Staphylococcal adhesion is inhibited by heparins but not by integrin blockade

Despite previous studies demonstrating the importance of β1 integrins for staphylococcal invasion of epithelial cells, RGD peptides, which inhibit integrin-ligand interactions, had no effect on staphylococcal adhesion to epithelial cells (Fig. 1B). A similar lack of effect was observed with various anti-α5β1 integrin antibodies (P1D6, Lia1/2, JBS5, and AIIB2) (Fig. S6). HSPGs have also been demonstrated to be involved in staphylococcal adherence to epithelial cells (5). Heparin and heparan sulfate have successfully been employed to block the binding of various pathogens to human cells (29). Here, we utilize UFH, dalteparin, and fondaparinux to interfere with the HSPGs. The differences between these compounds are defined in terms of their thrombin and anti-thrombin binding capabilities. UFH is a heterogenous mix of sulfated glycosaminoglycans (3–30kDa) able to bind both thrombin and antithrombin, while dalteparin is a low molecular weight heparin (LMWH)(4–6kDa) with the thrombin binding domain removed (30). Fondaparinux is a synthetic pentasaccharide based on the anti-thrombin binding region of heparin (31). In contrast to integrin blockade, WT cells treated with UFH had significantly reduced staphylococcal adherence at 10 I.U./mL (43.5 ± 2.2%; Fig. 1C and 2), confirming a role for HSPG in staphylococcal adhesion. This reduction by UFH was biphasic, with maximal inhibition at 50 I.U./mL but less effect at higher concentrations (Fig. 1C). Similar results were observed for the keratinocyte cell line, HaCaT, with staphylococcal adhesion recovering almost completely at higher concentrations of UFH (Fig. S5B). Interestingly, no effect of UFH was observed with CD9$^{-/-}$ cells (Fig. 1C), demonstrating a requirement for CD9 in UFH activity. UFH was inhibitory of staphylococcal growth at high concentrations (>80 I.U./mL), however, no effect was observed at concentrations which reduced adherence (Fig. S2C). Reductions in staphylococcal adherence to WT cells but not CD9$^{-/-}$ cells were also observed when cells were treated with the LMWH, dalteparin (Fig. 1D). However, fondaparinux did not appear to affect the adherence of *S. aureus* to WT or knockout cells (Fig. 1D), thus was used as a control in subsequent studies. Similar effects of 800C and UFH were observed if the number of bacteria associated with epithelial cells were enumerated by microscopy rather than by CFU (Fig. S5F). Infection with an *S. aureus* Δfnb deletion mutant, with both fibronectin binding protein A and B removed, demonstrated significantly reduced adherence to WT cells (Fig. 1E; 66.7 ± 3.1%). Removal of these adhesins completely ablated the effects of both 800C and UFH (Fig. 1E). Similar effects of 800C and UFH were also observed with primary normal human tonsillar keratinocytes that express high levels of CD9 and low levels of α5β1 and SDC-1 (Fig. 1F; Fig. S1D). Furthermore, 800C and UFH were also effective during infection of corneal and intestinal epithelial cell lines (Fig. S7), demonstrating the importance of both CD9 and HSPGs but not α5β1 integrin during staphylococcal adherence to a range of epithelial cell types.
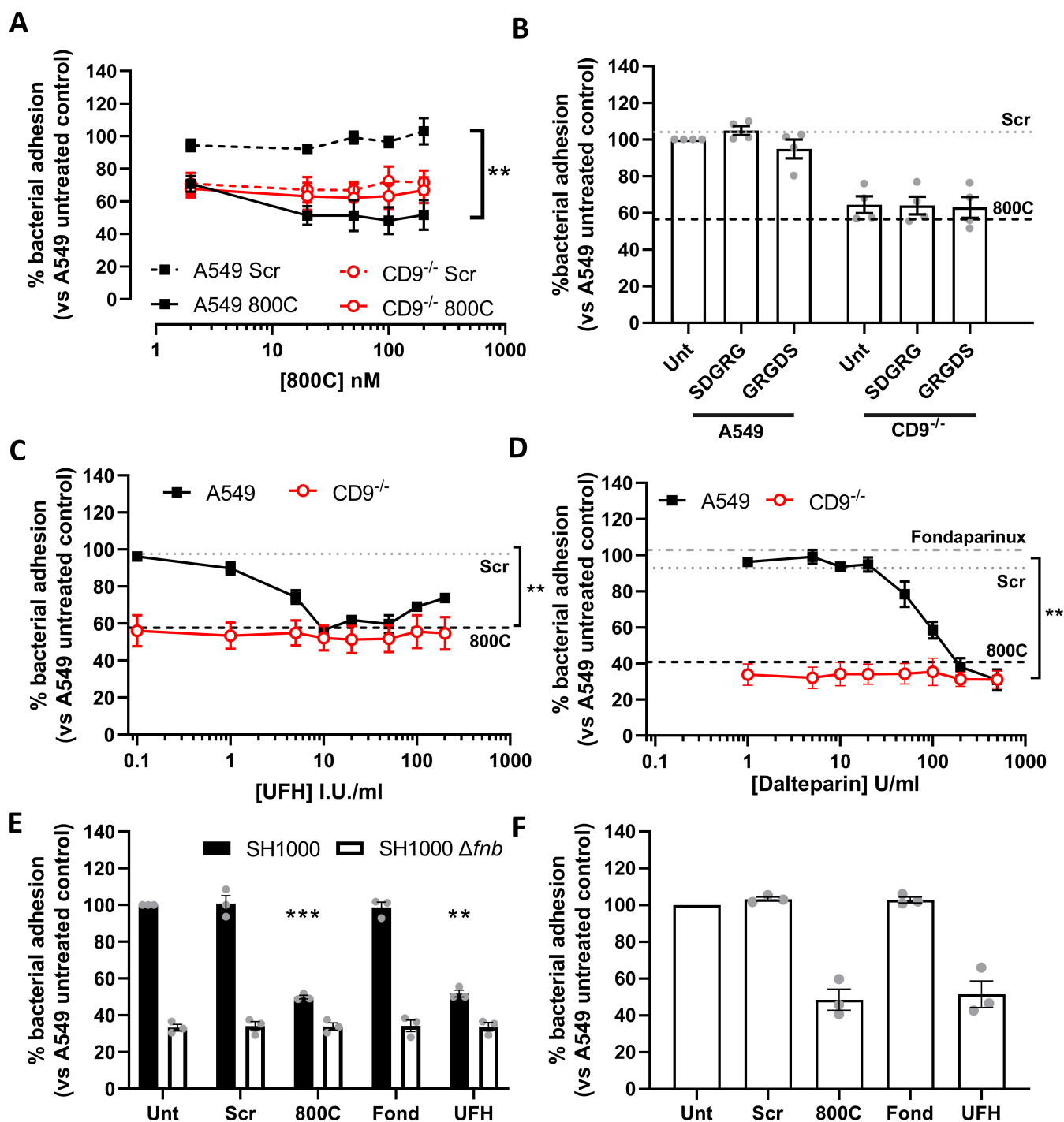
FIG 1 Tetraspanin derived peptides and heparin derivatives but not RGD peptides reduce staphylococcal adherence. Cells were infected with SH1000 for 60 min at an MOI = 50. (A) WT (black) or CD9$^{-/-}$ (red) cells treated with scrambled (dotted) or 800C peptide (solid) for 60 min prior to infection. WT (black) or CD9$^{-/-}$ (red) cells treated with RGD peptides (100 µM) (B), or various concentrations of heparin sodium (C) or dalteparin (D) for 60 min prior to infection. Effect of CD9-derived peptide treatment (200 nM) shown by dotted lines (B–D). Effect of fondaparinux (10 µg/mL) treatment on WT cells shown in panel D. (E) WT cells treated with scrambled peptide, 800C, fondaparinux, or UFH were infected with either SH1000 (black bars) or SH1000 Δfnb (white bars) for 60 min at an MOI = 50. (F) NTKs treated with scrambled peptide, 800C, fondaparinux, or UFH were infected with SH1000 for 60 min at an MOI = 50. $n \geq 3$, mean ± SEM, one-way ANOVA.
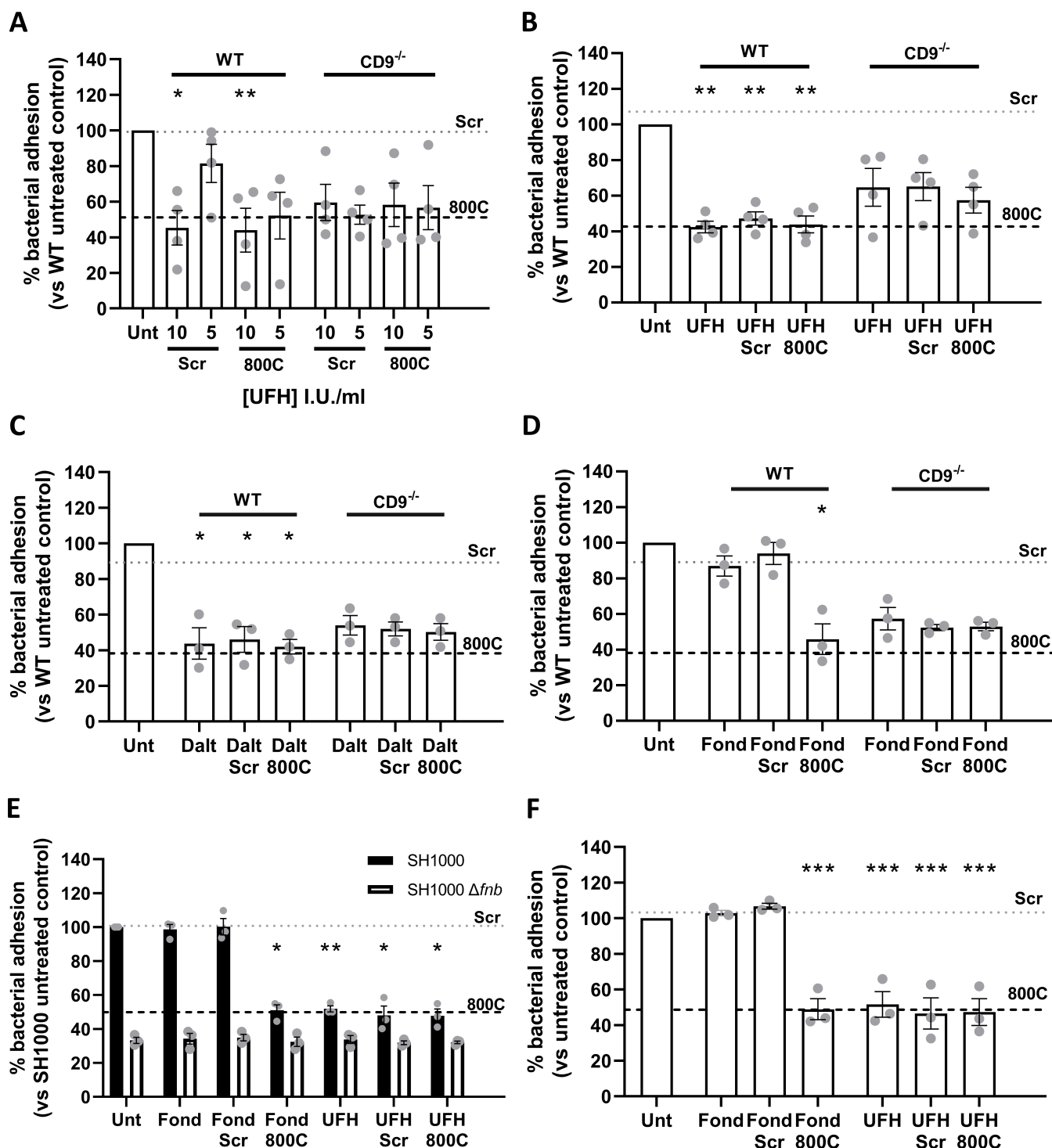
FIG 2 Combination treatment of unfractionated heparin and 800C produces no additive effects. Cells were infected with SH1000 for 60 min at an MOI = 50. (A) WT or CD9$^{-/-}$ A549 cells were treated with UFH, 800C peptide, or a combination of both for 60 min prior to treatment. (B) WT or CD9$^{-/-}$ A549 cells were treated with peptide (200 nM) for 60 mins prior to infection. UFH (10 U/ml), either in combination with 800C peptide or as a singular treatment, was added at the start of infection. (D) WT or CD9$^{-/-}$ cells were treated with fondaparinux (10 µg/mL), 800C peptide (200 nM), or a combination of both 60 min prior to infection. (E) WT cells treated with 800C peptide (200 nM), UFH (10 U/mL), or a combination of the two and infected with either SH1000 or SH1000 Δfnb at an MOI = 50. (F) NTKs treated with 800C peptide (200 nM), UFH (10 I.U./mL) or a combination of the two and infected with SH1000 for 60 min at an MOI = 50. $n \geq 3$, mean ± SEM, and one-way ANOVA.

Heparin and CD9-derived peptides affect similar staphylococcal adherence pathways

The lack of effect of heparin and its analogs and 800C in CD9$^{-/-}$ cells together with the observation that these treatments all reduce staphylococcal adherence to similar levels with WT cells (Fig. 1) suggests that these treatments affect similar pathways. We, therefore, tested 800C and the various heparin analogs in combination to test for additive effects. WT cells pre-treated with a combination of scrambled peptide and 10 I.U./mL UFH before infection demonstrated a significant reduction in staphylococcal adherence (54.7 ± 19.4%); as expected these effects were smaller when treated with 5 I.U./mL of UFH (Fig. 2A). When UFH was combined with 800C, staphylococcal adherence was reduced to similar levels as either treatment alone (51.1 ± 20.9%) with no evidence of a synergistic effect and no effect of either treatment with CD9$^{-/-}$ cells (Fig. 2A). When WT cells were pre-treated with scrambled peptide and UFH was added during the infection, similar reductions in staphylococcal adherence were observed when treated with UFH or 800C alone (52.2 ± 7.5%; Fig. 2B). A combined treatment of UFH and 800C on WT cells caused no further additional effects while treatment of CD9$^{-/-}$ cells had no effect (Fig. 2B). Similarly, pre-treatment of cells with LMWH dalteparin and scrambled peptide reduced staphylococcal adherence to similar levels as cells pre-treated with 800C or dalteparin alone (54.0 ± 12.5%; Fig. 2C). Combination treatment of dalteparin and 800C had no further additive effect and treatments had no effect on CD9$^{-/-}$ cells (Fig. 2C). Pre-treatment of cells with scrambled peptide and fondaparinux demonstrated no significant reductions in staphylococcal adherence and, when combined with 800C, adherence was reduced to levels similar to that of 800C treatment alone (54.2 ± 14.9%; Fig. 2D). No effects of either treatment were observed with CD9$^{-/-}$ cells or when WT cells were infected with a Δ*fnb* mutant (Fig. 2E). Similarly, no additive effects were observed after a combined treatment of UFH and 800C on normal tonsillar keratinocytes (NTKs) (Fig. 2F). Thus, CD9 has been implicated within the same staphylococcal adherence pathway as the HSPGs in epithelial cells for the first time.

Heparan sulfates are required during tetraspanin-mediated staphylococcal adherence

Reductions in staphylococcal adherence by both 800C and heparin analogs suggest that HSPGs are involved during tetraspanin-mediated staphylococcal adherence. To further test this, adherence of *S. aureus* to epithelial cells was measured after removal of the major decorating sugar groups, HS or CS, from the cell surface using heparinases and chondroitinases, respectively. Treatment with a mixture of heparinase I/III significantly reduced staphylococcal adherence to WT cells (53.1 ± 13.7%), while combination treatment with scrambled peptide or 800C had no further additive effect (Fig. 3A). Treatment of WT cells with chondroitinase ABC (Fig. 3A) did not reduce staphylococcal adherence. No significant reduction was observed when CD9$^{-/-}$ cells were treated with heparinase or chondroitinase (Fig. 3B). Staphylococcal adherence was also significantly reduced when cells were pre-treated with 10 µg/mL HS (37.3 ± 4.2%; Fig. 3C) or DS (42.1 ± 3.4%; Fig. 3D). As with heparin, treatment of CD9$^{-/-}$ cells with HS or DS did not reduce staphylococcal adherence (Fig. 3C and D). CS treatment had no effect on WT or CD9$^{-/-}$ cells (Fig. 3E). Treatment with pixatimod, a clinical stage HS mimetic (32), also caused a significant reduction in staphylococcal adhesion to WT cells (42.4 ± 4.5%) but not CD9$^{-/-}$ cells (Fig. 3F). This suggests the importance of HS chains but not the core protein of HSPGs, during CD9-mediated staphylococcal adherence, and demonstrates a potential new therapeutic to interfere with this process.

Tetraspanin-mediated staphylococcal adherence requires SDC-1

Removal of HS from HSPG and treatment with heparin analogs or with HS all reduce staphylococcal adherence in a similar manner to 800C, suggesting the involvement of HSPGs in tetraspanin-mediated adherence. A number of HSPGs have been demonstrated
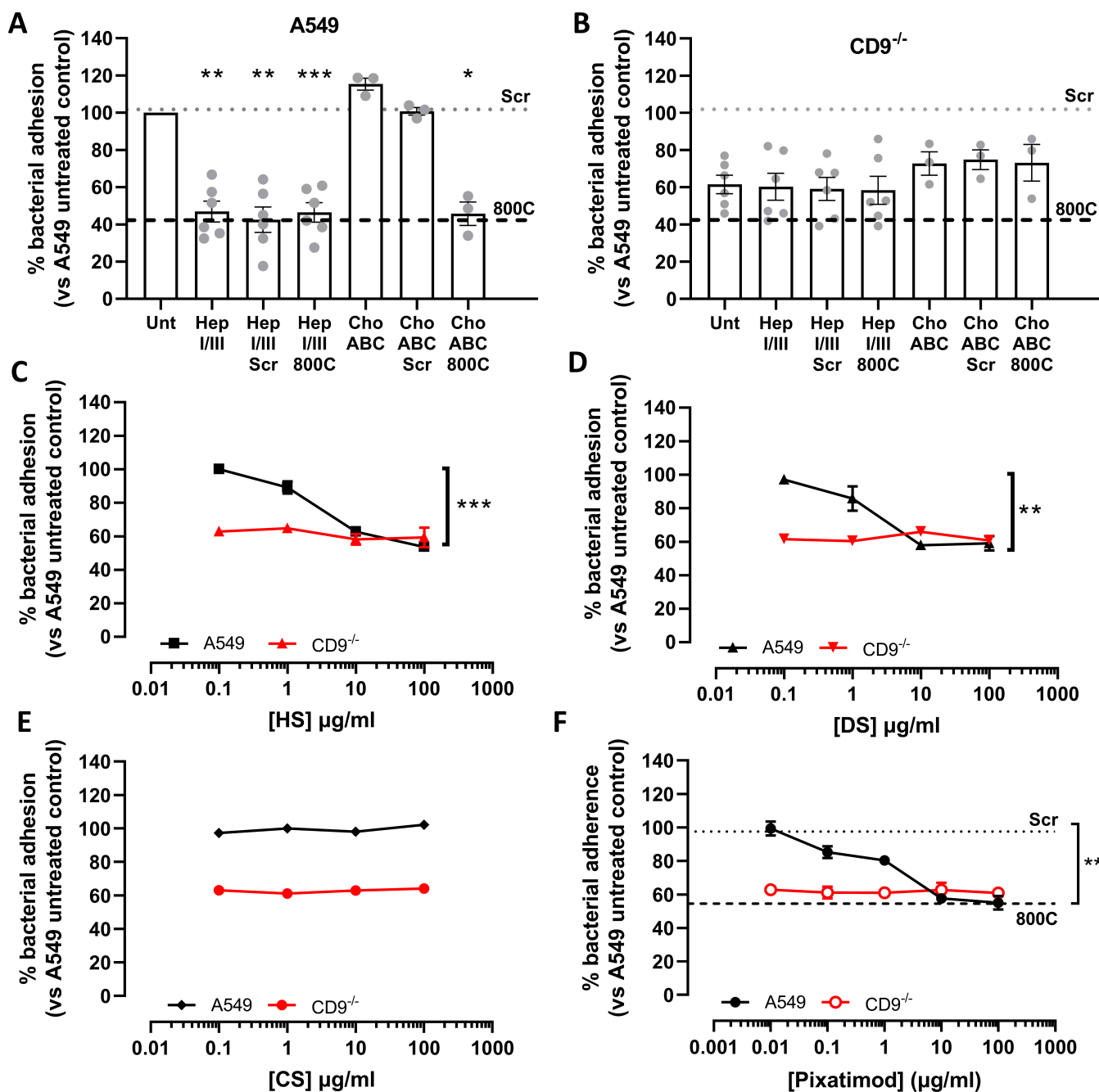
FIG 3 Heparan sulfates are required during tetraspanin-mediated staphylococcal adherence. Cells were infected with SH1000 for 60 min at an MOI = 50. (A) WT cells were treated with either 0.25 U/mL chondroitinase ABC or 0.5 U/mL heparinase I/III for 3 h prior to infection. Peptide was added to cells 60 min prior to infection for combination treatments. (B) CD9$^{-/-}$ cells were treated with either 0.25 U/mL chondroitinase ABC or 0.5 U/mL heparinase I/III for 3 h prior to infection. Peptide was added to cells 60 min prior to infection for combination treatments. WT or CD9$^{-/-}$ cells were treated with heparan sulfate (HS; C), dermatan sulfate (DS; D), chondroitin sulfate (CS; E), or the heparan sulfate mimetic (pixatimod; F) for 60 min prior to infection. $n \geq 3$, mean ± SEM, and one-way ANOVA.

to associate with CD9, including SDC-1 (33). Syndecans are expressed on epithelial cells, with SDC-1 and SDC-4 being the most abundant (34). Here, we tested the involvement of SDC-1 and SDC-4 in this process using blocking antibodies and shRNA knockdowns. Both SDC-1 and SDC-4 were expressed on WT cells, with SDC-1 expression higher than SDC-4 (Fig. S1A). Staphylococcal adherence was reduced after treatment with an anti-SDC-1 antibody (46.6 ± 3.3%) similar to treatment with 800C, but no effect was observed if WT cells were treated with an isotype control antibody (Fig. 4A). No further additive effect
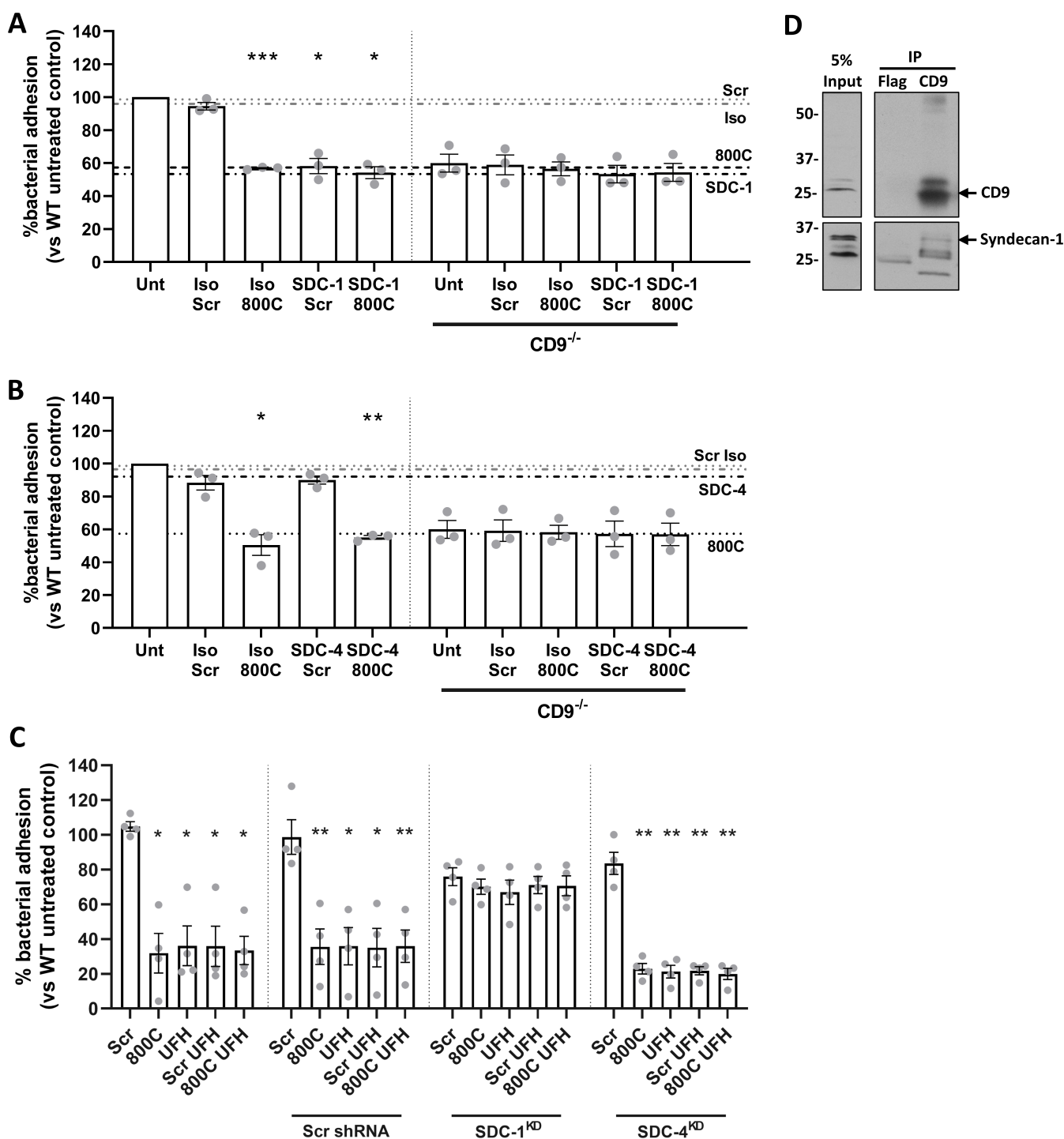
FIG 4 Syndecan-1 is involved in tetraspanin-mediated staphylococcal adherence to epithelial cells. Cells were infected for 60 min with SH1000 at an MOI = 50. (A) WT or CD9$^{-/-}$ cells were treated with peptides (200 nM), isotype control (JC1), anti-SDC-1 antibodies (B-A38, 10 µg/mL), or a combination of peptide and antibodies for 60 min prior to infection. (B) WT or CD9$^{-/-}$ cells were treated with peptides (200 nM), isotype control (02–6200), anti-SDC-4 antibodies (5G9, 20 µg/mL), or a combination of peptide and antibodies for 60 min prior to infection. (C) shRNA knockdowns of SDC-1 and SDC-4 were treated with peptides (200 nM), UFH (10 I.U./mL), or a combination of the two for 60 min prior to infection. Scrambled shRNA was used as a control. $n \geq 3$, mean ± SEM, and one-way ANOVA. (D) Whole cell lysates were immunoprecipitated with anti-CD9 antibodies (MM2/57), and the resulting elutes were probed with either anti-CD9 or anti-SDC-1 antibodies. Lysates were probed with anti-FLAG antibodies as a control.
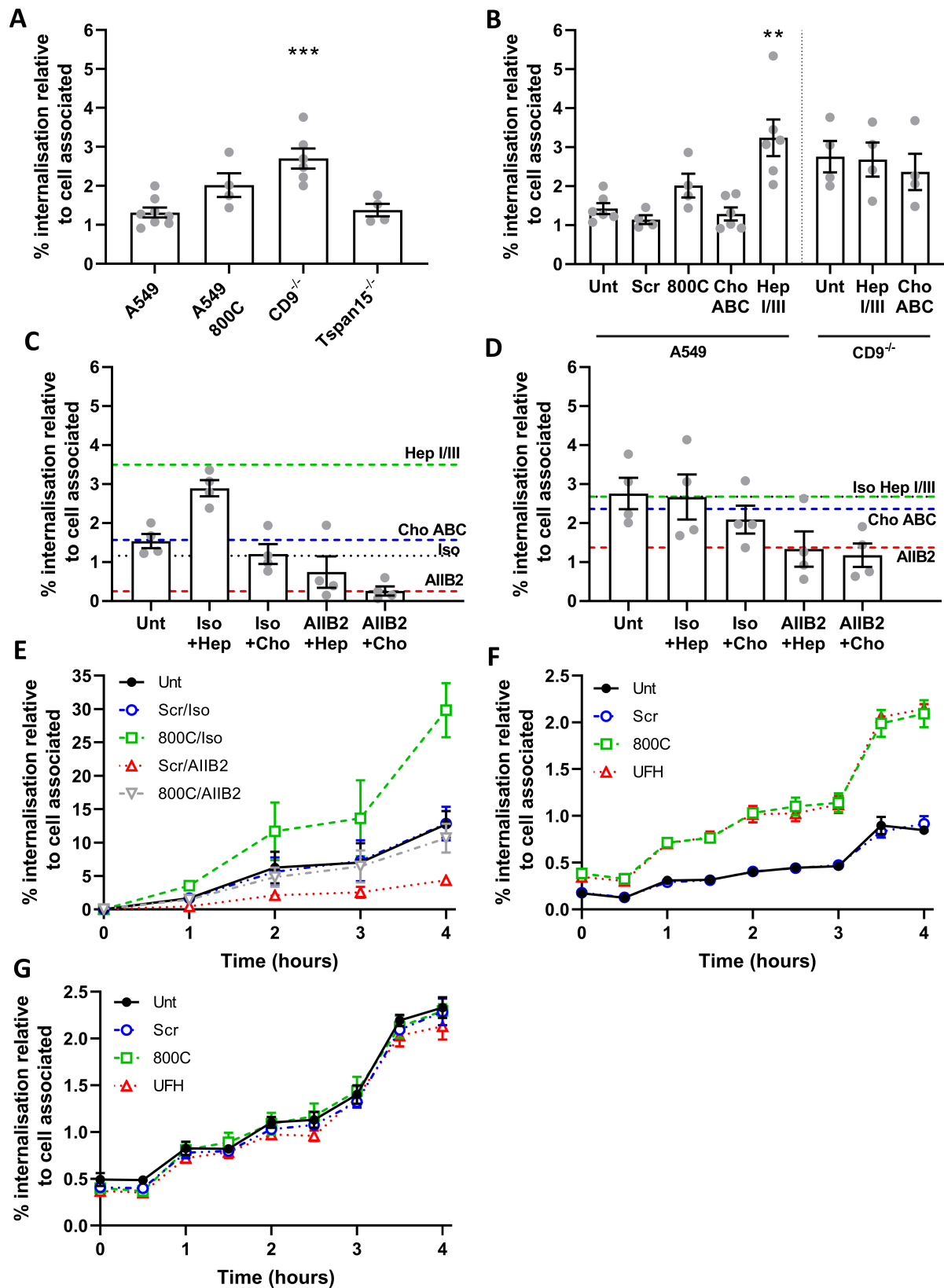
FIG 5 Interference with CD9 or heparan sulfates increases staphylococcal internalization, which is controlled by α5β1. Cells were infected with SH1000 for 60 min at an MOI = 50. After infection, cells were washed and treated with 200 µg/mL gentamicin sulfate to remove adherent bacteria and lysed to quantify the internalized bacteria. Internalized bacteria were normalized against the cell associated bacteria. (A) Internalized bacteria within WT, CD9$^{-/-}$, and Tspan15$^{-/-}$ cells, (Continued on next page)

FIG 5 (Continued)

800C treated WT cells are added as an example. (B) WT or CD9⁻/⁻ cells were treated with 0.25 U/mL chondroitinase ABC or 0.5 U/mL heparinase I/III for 3 h prior to infection. WT (C) or CD9⁻/⁻ (D) cells were treated with heparinase I/III or chondroitinase ABC for 3 h. Cells were treated with isotype control or anti-α5β1 antibodies (AIIB2) for 60 min prior to infection. (E) Cells were treated with combinations of peptide (200 nM), isotype control, and anti-α5β1 antibodies (AIIB2) for 60 min prior to infection. Cells were infected for 60 min at 4°C, after infection cells were warmed to 37°C and internalization was allowed to continue for 4 h. WT (F) or CD9⁻/⁻ (G) cells were treated with scrambled peptide (blue) (200 nM), 800C (green) (200 nM), or UFH (red) (10 I.U./mL) for 60 min prior to infection. Cells were infected for 60 min before being washed and treated with 200 µg/mL gentamicin sulfate. Internalized bacteria were allowed to grow for a further 4 hours before cells were lysed and enumerated. $n \geq 3$, mean ± SEM, and one-way ANOVA.

was observed if the anti-SDC-1 antibody was added in combination with 800C, while antibody treatment of CD9⁻/⁻ cells had no effect (Fig. 4A). Anti-SDC-4 antibodies had no effect on staphylococcal adherence (Fig. 4B). Partial knockdown of either SDC-1 or SDC-4 was very efficient (Fig. S8) but each had only small inhibitory effects on staphylococcal adherence to epithelial cells (29.6 ± 9.4% and 19.0 ± 10.1%, respectively) (Fig. S1C), suggesting some redundancy between the SDCs. However, knockdown of SDC-1 negated the effects of 800C and UFH on WT cells relative to untreated or scrambled shRNA treated cells whereas 800C and UFH were still effective at reducing staphylococcal adherence to SDC-4 knockdown cells (77.1 ± 6.0% and 78.7 ± 7.4%, respectively) (Fig. 4C). Co-immunoprecipitation of endogenous CD9 demonstrated direct association of CD9 with SDC-1 (Fig. 4D) confirming previous data (33). Thus, SDC-1 appears to be the primary membrane protein required for CD9-mediated staphylococcal adhesion.

Interference with HSPGs and CD9-derived peptide increases staphylococcal internalization

We have demonstrated that staphylococcal adherence can be reduced by interfering with HSPGs and CD9 but not by blockade of β1 integrins. Here, we tested the effects of these treatments on the internalization of *S. aureus* into epithelial cells using a gentamicin protection assay. For CD9⁻/⁻ cells, internalization of adherent bacteria was significantly increased (2.7 ± 0.6%; $P = 0.0001$) compared to WT cells (1.4 ± 0.34%) (Fig. 5A). A similar increase was observed with WT cells treated with 800C (2.0 ± 0.6%); however, this did not reach significance ($P = 0.094$) (Fig. 5A). Although smaller than in CD9⁻/⁻ cells, a reduction was also observed in cell-associated bacteria in Tspan15⁻/⁻ cells (Fig. S1C), however, no increase was observed in internalization (Fig. 5A) suggesting that internalization is CD9 specific and not due to changes within the number of cell-associated bacteria. Increases in internalization were also observed in WT cells treated with heparinase I/III (3.2 ± 1.2%) but not with chondroitinase ABC (Fig. 5B), whereas no further increases were observed for CD9⁻/⁻ cells treated with heparinase I/III (Fig. 5B). Treatment of WT cells with AIIB2, an antibody able to dissociate β1:Fn complexes, reduced internalization to negligible levels (0.3 ± 0.2%), while treatment of CD9⁻/⁻ cells with AIIB2 only reduced internalization to levels observed in untreated WT cells (Fig. 5C and D). Increases in internalization were observed for 4 h after infection (Fig. 5E), although increasing cell death prevented measurement after this point. Treatment of WT cells with a combination of a scrambled peptide with AIIB2 reduced internalization to very low levels throughout, similar to the AIIB2 alone (Fig. 5E). Interestingly, treatment of WT cells with a combination of 800C and AIIB2 reduced tetraspanin-mediated internalization back to levels observed with untreated WT cells at all time points (Fig. 5E), suggesting that β1:Fn complexes are still critical for internalization of *S. aureus* even in the absence of CD9. Similarly, if AIIB2 is used in combination with heparinase treatments, internalization is reduced to untreated levels (0.8 ± 0.8%; Fig. 5D). This effect is not due to differences in the growth of internalized bacteria as this is minimal over a 4h period and does not account for the increased levels of internalization (Fig. 5F and G). While more bacteria were detected in 800C and UFH treated cells or CD9⁻/⁻ cells, this is due primarily to increased internalization as growth rates of all treatments remained the same, increasing by approximately fivefold over 4 h (Fig. 5F and G). These data indicate that CD9 is a positive regulator of HSPGs during initial adherence but that CD9 is a negative regulator

of the subsequent α5β1-mediated internalization, suggesting that CD9 links these two separate events.

Changes in the expression of SDCs and α5β1 integrin do not explain the reduced staphylococcal adherence in CD9 knockout cells

The expression of α5β1 integrins and the SDCs was measured by flow cytometry in CD9$^{-/-}$ cells to determine if the effect on staphylococcal adherence is secondary to changes in expression of these membrane proteins. As expected for CD9$^{-/-}$ cells, CD9 expression was dramatically reduced compared to WT cells (−73.3 ± 1.5%; Fig. 6A) with the number of positive cells reduced by 95.4 ± 0.5% (Fig. S1B). Surprisingly, both SDC-1 and SDC-4 demonstrated increased expression on CD9$^{-/-}$ cells relative to WT (117.5 ± 25.8% and 21.6 ± 11.3%, respectively) although the number of SDC-4 positive cells dropped markedly (50.8 ± 5.8%) (Fig. S1B). Integrin α5 and β1 expression was measured with two separate antibodies; AIIB2 is able to dissociate β1:Fn interactions and can therefore measure total surface β1, and JBS5 is unable to dissociate these interactions and so only measures the unliganded fraction of α5 (35). Interestingly, JBS5 binding was reduced in CD9$^{-/-}$ cells relative to WT (−44.9 ± 15.0%; Fig. 6A), with the percentage of positive cells also reduced (−89.9 ± 1.8%), while AIIB2 binding was increased in the CD9$^{-/-}$ cells (9.9 ± 9.0%) (Fig. S1B). Taken together, these data suggest that CD9 can regulate cell surface expression of SDCs, but SDC expression levels are not the critical determinant of staphylococcal adherence. CD9 may also act to keep a population of α5β1 in an inactive state unable to bind Fn.

Fn is important for tetraspanin-mediated staphylococcal adherence

As differences were observed in cell surface proteins known to bind extracellular matrix proteins, we tested whether bacterial adherence could be affected by the addition of exogenous Fn. The addition of Fn to WT cells increased staphylococcal adherence in a dose-dependent manner, with only low concentrations of Fn required to increase S. aureus binding to WT cells (EC$_{50}$ = 6.3 µg/mL, Fig. 6B). However, a much higher concentration of Fn is required to increase staphylococcal adherence to CD9$^{-/-}$ cells (EC$_{50}$ = 747.9 µg/mL) (Fig. 6B). Adherence by the Δfnb mutant remained unaffected by the addition of exogenous fibronectin (Fig. 6B). These data cannot be explained by increases in bacterial binding to Fn in the absence of cells (Fig. S9A). To further test the importance of CD9 during increased binding of S. aureus after addition of exogenous extracellular matrix proteins, we tested 800C in combination with 10 µg/mL Fn and observed a reduction in staphylococcal adherence (51.5 ± 22.4%) to levels similar to that of 800C treatment alone, despite the increases observed if Fn was added alone (175 ± 7.20%) or in combination with the scrambled peptide (172 ± 9.10%) (Fig. 6C). No effect of Fn or 800C was observed with CD9$^{-/-}$ cells (Fig. 6C) or after infection with a Δfnb mutant (Fig. S9B). Interestingly, addition of UFH, Fn, or collagen to bacteria prior to infection had no effect on staphylococcal adherence to cells although adherence of Fn or collagen-treated bacteria was significantly reduced after treatment with 800C (44.8 ± 21.8% and 49.4 ± 33.7%, respectively) (Fig. 6D). However, the effect of 800C was completely abrogated when cells were infected with UFH treated bacteria (Fig. 6D). Taken together, this suggests a significant role for Fn during CD9-mediated staphylococcal adherence.

DISCUSSION

In this study, we have identified a critical role for CD9 in the control of the behavior of SDC-1-dependent S. aureus adhesion sites. Integrin α5β1 plays no part in this adherence pathway but does have a role in the subsequent internalization of bacteria. Interference with CD9/SDC-1 led to increases in internalization that were reduced by integrin blockade, suggesting a sequential CD9-mediated process connecting adherence with internalization. The addition of exogenous Fn increased binding in a CD9-sensitive manner, suggesting the importance of Fn during tetraspanin-mediated adherence, likely
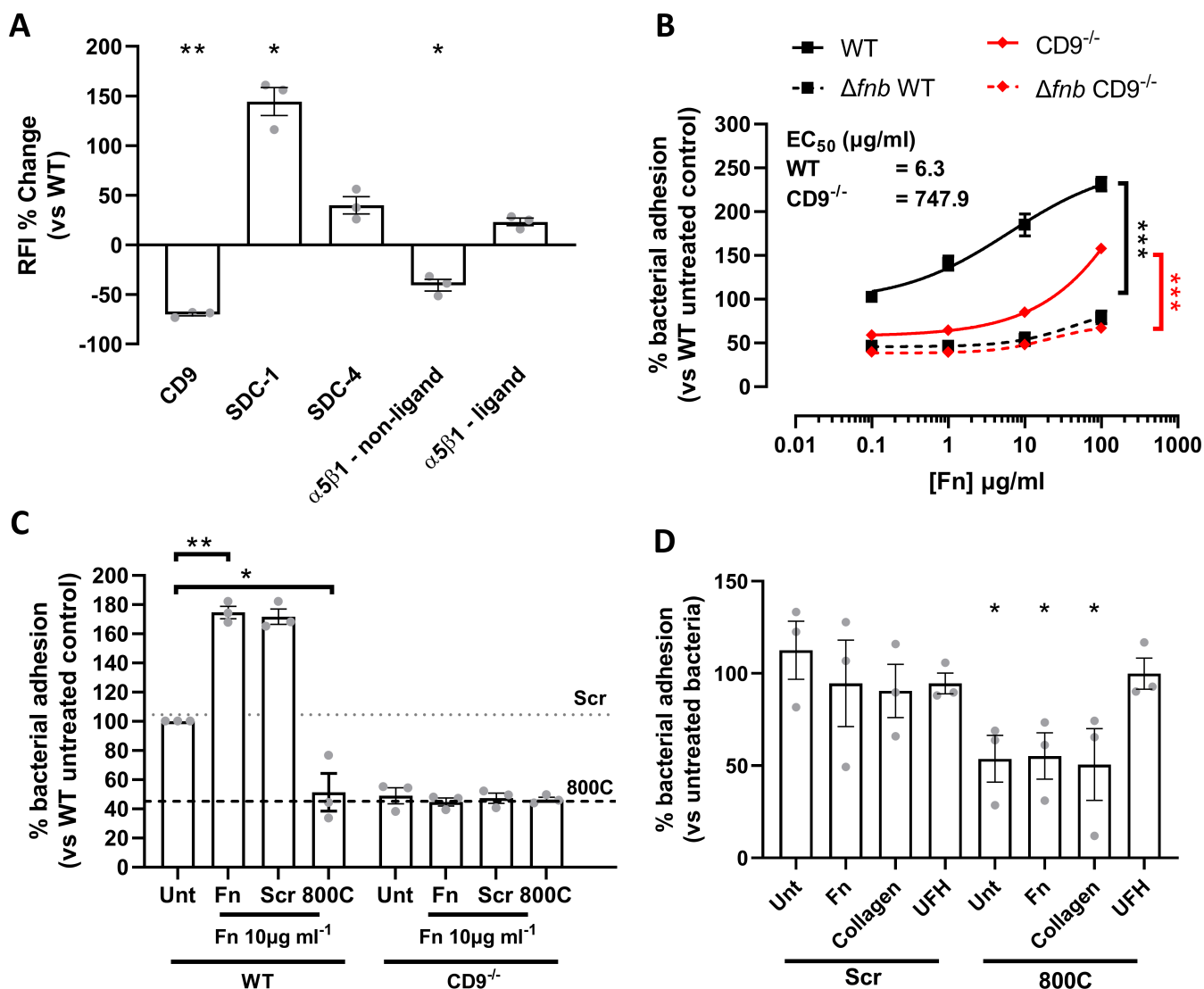
FIG 6 Addition of exogenous Fn increases staphylococcal adherence, which is negated in the presence of 800C. (A) Cell surface expression of receptors of interest was determined in CD9$^{-/-}$ cells. Relative fluorescence intensity was calculated by dividing the test antibody by the isotype control. Percentage change was calculated against WT cell values. (B) Cells were treated with varying concentrations of Fn prior to infection with SH1000 or SH1000 Δfnb. (C) Fn was added to WT or CD9$^{-/-}$ cells in combination with 800C or a scrambled peptide for 1 h prior to infection. (D) SH1000 was pre-treated with Fn, collagen, or UFH for 90 min prior to infection. Cells were treated with 200 nM 800C or scrambled peptide for 60 min prior to infection. $n \geq 3$, mean ± SEM, and one-way ANOVA.

by integration with CD9/SDC-1. Finally, we present two potential anti-adhesive therapeutics, CD9-derived peptide 800C and heparin, providing a mode of action for both.

A new model for staphylococcal adhesion to epithelial cells

Our studies demonstrating the interaction of CD9 with syndecan-1 by co-immunoprecipitation, alongside similar studies that also show CD9 interaction with α5β1 (33, 36), lead us to propose the following model (Fig. 7), in which CD9 TEMs contain either SDC-1 or α5β1. Clustering of SDC-1, within CD9 enriched microdomains, leads to recruitment and organization of Fn fibrils into "adhesion nets" on the cell surface (12, 37) increasing bacterial adherence. CD9-blockading reagents, such as 800C and antibodies, may operate by disrupting CD9-containing TEMs and, therefore, the organization of Fn fibrils by TEM-associated SDC-1. Treatment with UFH or heparin derivatives may also disrupt the established fibronectin adhesion net (38) or block staphylococcal association to Fn (39), therefore, reducing bacterial adhesion efficiency. 800C and UFH treatments were

both able to reduce staphylococcal adherence by approximately 50–60%, demonstrating that other adherence pathways, which may utilize other bacterial adhesins, remain unaffected by these treatments. We have demonstrated this in epithelial cells from multiple physiological locations, including tonsillar tissue, keratinocytes, and the cornea, suggesting that this mechanism is conserved across various potential infection sites.

The role of syndecans in staphylococcal adhesion

Our findings add to others that have implicated HSPGs, and particularly SDC-1, in the staphylococcal adherence pathway (5, 7, 8). However, some studies have suggested that while SDC-1 is important for staphylococcal infection, it is not a direct receptor. For example, Hayashida et al. demonstrated a lower burden of staphylococcal corneal infection in Sdc1$^{-/-}$ knockout mice but did not observe interaction of S. aureus with SDC-1 on beads or with a mouse SDC-1 knockdown corneal epithelial cell line (9). They instead suggest that S. aureus induction of SDC-1 ectodomain shedding, likely through the action of ADAMs (a disintegrin and metalloproteinase) or other metalloproteinases, is critical for improved survival of the bacteria. SDC-1 ectodomains have been shown to inactivate cathelicidins and reduce neutrophil-mediated killing, significantly increasing staphylococcal survival during infection (40, 41). The association of tetraspanins with syndecans and ADAMs suggest that tetraspanins may also be involved in ectodomain shedding. Further studies investigating the role of CD9 in ADAM-mediated ectodomain shedding could provide valuable data into tetraspanin control of another putative pathogenesis pathway. However, we would further suggest the expression profile between the cell lines used and those in this study differ significantly with lower levels of CD9 potentially reducing clustering of receptors and so lowering the avidity of interactions between S. aureus and SDC-1. This study has utilized multiple cell lines that show both differences in staphylococcal adhesion and protein expression profile (Fig. S7). Furthermore, while we have shown that SDC-1 appears to be important during tetraspanin-mediated adhesion, we also observed an increase in SDC-1 expression on CD9$^{-/-}$ cells (Fig. 6A), to which staphylococcal adhesion is also significantly reduced suggesting that coordination and clustering of this HSPG are important.

Other studies suggest that the primary role of SDC-1 is the organization of Fn at the host cell surface, through the GAG binding domains of Fn (12). Various bacteria are then able to interact directly with Fn through FnBPs located in their outer membrane (42). Our data suggest that the coordinate action of CD9 and SDC-1 is required for efficient staphylococcal adherence, whereby CD9 clusters SDC-1 in TEMs to allow the organization of Fn into adhesion platforms. However, we cannot rule out that a specific moiety of HS is required on SDC-1 for adherence, as we demonstrate that HS as well as DS, which both decorate syndecans, reduce staphylococcal adherence to a similar extent as 800C. While we have not investigated other HSPGs such as the glypicans. These GPI-anchored proteins are usually present in lipid rafts (43), unlike the syndecans that have been associated with TEMs (33, 44), and so glypicans are less likely to be involved in these processes. Furthermore, the equivalent effects of heparins and the CD9-derived peptide, together with the abrogation of these effects on SDC-1 knockdown, suggest that the glypicans cannot replace SDC in this tetraspanin-mediated adherence pathway.

The role of integrins in staphylococcal adhesion and internalization

Syndecans and integrins interact with Fn and other extracellular matrix proteins to provide structural support enabling cell:cell adhesion and transmembrane interactions for downstream cell signaling (45). Both families of proteins have been implicated in Fn fibril assembly, a process thought to require co-localization and clustering of these proteins (37, 46, 47). Loss of SDC-1 in corneal cells led to less activated β1 integrin, which was used to explain reduced Fn fibril formation (37). In addition, expression of CD9 on Chinese hamster ovary cells led to reduced cell adhesion and increased spreading on Fn (48), with CD9 expression proposed to stabilize the "active" conformation of α5β1 (49). Interestingly, Cook et al. found that a 37 aa peptide derived from the CD9 EC2, containing
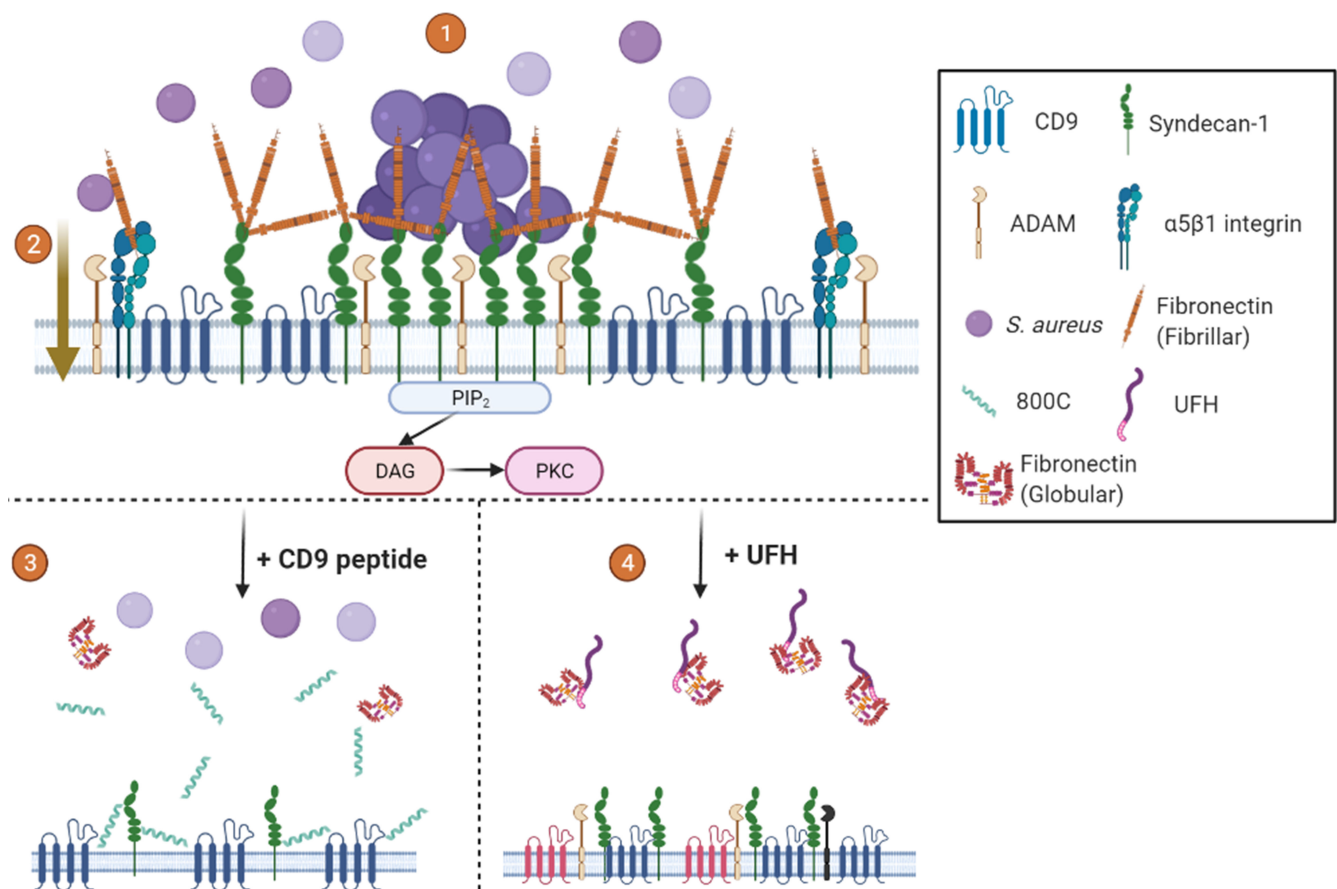
FIG 7 Proposed mechanism for tetraspanin-mediated staphylococcal adherence. (1) CD9 enriched microdomains contain syndecan-1. Clustering of syndecan-1 by CD9 recruits fibronectin and produces "adhesion nets". *S. aureus* utilizes these nets to initiate initial adherence to the cell surface (2). Inclusion of integrins in CD9 enriched microdomains means the "adhesion nets" are in close proximity to β1 integrins, allowing for the transfer of bacteria after initial adherence for rapid internalization through the canonical pathway. Interactions with CD9 and ADAMs ensure integrins are kept in an inactive state inhibiting bacterial internalization (3). CD9-derived peptides increase the area of TEMs pushing syndecan clusters apart and reducing the formation of "adhesion nets" (4). UFH treatment displaces fibronectin or blocks staphylococcal interaction with Fn, destabilizing TEMs and reducing bacterial adhesion. Mechanisms other than CD9-mediated adhesion and internalization are still possible with both treatments. Created with Biorender.com.

the sequence utilized in the present study, was able to reverse the inhibition of CHO cell adhesion to Fn (50). However, our data suggest that CD9-mediated SDC clustering may provide an indirect link between CD9 and Fn. CD9 has also been shown to negatively regulate cell adhesion by promoting the interaction of α5β1 with ADAM17, keeping both molecules in an inactive state (36). No change in the activation state of α5β1 was observed, but α5β1 shifted from an equal distribution pattern on the cell surface to more punctate clusters in the absence of CD9 (36). The FnBPs of *S. aureus* are known to drive the clustering of integrins upon interaction with Fn, which leads to rapid internalization (51). The present study focuses on changes within host adhesion receptors but poses intriguing questions as to the role of *fnbA* and *fnbB* within tetraspanin-mediated staphylococcal adhesion. Here, we showed that ligand-bound β1, suggesting an "active" integrin conformation, increased in the absence of CD9; however, this was accompanied by higher expression of SDC-1. We also observed greater staphylococcal adherence in the presence of Fn, which was abrogated by the CD9-derived peptide, and increased internalization with the loss of CD9 or after interference with HSPGs. Recently and in agreement with our studies, the supramolecular structure of fibronectin at the cell surface has been linked to differential uptake of *S. aureus* (52). A denser, layered Fn fibril network at the surface of osteoblasts demonstrated a poorer uptake of bacteria compared to a moderate Fn fibril network at the surface of A549 epithelial cells suggesting

that an optimal concentration and organization of Fn is required for efficient adhesion and uptake. Furthermore, and also in agreement with our results, a recent study has demonstrated that anti-α5β1 antibodies demonstrate no effect on staphylococcal adhesion but abrogate internalization (53). We, therefore, suggest that clustering of SDC-1 by CD9 and the resulting Fn fibril formation drives the initial adherence of *S. aureus*. These bound bacteria are then able, through the action of FnBPs, to begin clustering of α5β1 and thus promote internalization over adherence.

The potential of CD9 peptides and heparins as anti-infective agents

We have provided insights into the mode of action of a new anti-bacterial adhesive therapeutic, 800C, suggesting that it may disrupt SDC-1 clusters that act as the anchor of "adhesion nets" on the cell surface, significantly inhibiting staphylococcal adherence to a variety of host cell types. Future studies will investigate analogs of 800C to further reduce staphylococcal adherence and to check safety and efficacy of tetraspanin-derived peptide treatments. We have recently demonstrated that a stapled form of 800C is effective in *in vivo* and *ex vivo* models of infection with no detrimental effects to the host (54). UFH and heparin analogs have previously been demonstrated to inhibit the adherence of various bacteria and viruses (29). Our study adds significantly to the growing body of evidence that suggests heparin could be used as an anti-adhesive therapeutic and provides a mechanism for its mode of action. Previously thought to interact directly with some bacterial adhesins (6) or with fibronectin (39), our data suggest that heparin also acts on the host via the SDC/CD9/Fn "adhesion net". While we observed a biphasic response of UFH upon staphylococcal adherence suggesting that heparin may be directly utilized by the bacteria at higher concentrations (55), we also demonstrated inhibitory effects of low molecular weight heparins. However, typical therapeutic serum concentrations of LMWH are 0.5–1.2 U/mL (30), much lower than the inhibitory concentrations required in this study (Dalteparin IC_{50} = 85.2 U/mL). Fondaparinux, a synthetic pentasaccharide heparinoid able to bind antithrombin but not thrombin (31), showed little effect here, providing an insight into the structural requirements for a heparin-based anti-infective. We have also demonstrated for the first time significant inhibition of staphylococcal adherence using Pixatimod (PG545, IC_{50} = 1.11 µg/mL), a clinical stage HS-mimetic that shows potent anti-cancer and anti-inflammatory effects (56). Pixatimod has also been reported to have significant anti-viral activity against a range of viruses which utilize HS as receptors including SARS-COV-2, HSV-2, HIV, RSV, and dengue (57–61). The emergence of new HS mimetics with significantly reduced anticoagulant activity suggests new avenues of research to develop anti-adhesive therapeutics against existing and emerging pathogens.

In summary, we have made the novel observation that the presence of CD9 at the cell surface, alongside SDC-1 and the integrins, is a critical component of a major mechanism of *S. aureus* adherence to epithelial cells from various physiological sites. We have also demonstrated the importance of Fn for CD9/SDC-1-mediated staphylococcal adherence and present two potential therapeutic pathways to significantly reduce staphylococcal adherence, namely CD9-derived peptides and heparin/HS analogs. With this study providing mechanistic details as to the action of these putative therapeutics, future studies should now investigate analogs which could further reduce staphylococcal adherence beyond the levels of inhibition demonstrated here. Previous data have suggested tetraspanin involvement in the adherence of a wide variety of Gram-positive and Gram-negative bacterial pathogens and so further investigations may shed light on a common pathway for bacterial pathogenicity involving the organization of HSPGs by tetraspanins. Furthermore, the tetraspanins are associated with and organize a number of different partner proteins that may act as bacterial host receptors; continued research may reveal more potential therapeutics relieving the burden during the antimicrobial resistance crisis.

ACKNOWLEDGMENTS

AUTHOR AFFILIATIONS

[1]Department of Infection, Immunity and Cardiovascular Disease, University of Sheffield Medical School, Sheffield, United Kingdom

[2]School of Biosciences, University of Sheffield, Sheffield, United Kingdom

[3]Department of Oncology and Metabolism, University of Sheffield Medical School, Sheffield, United Kingdom

[4]Department of Chemistry, University of Sheffield, Sheffield, United Kingdom

PRESENT ADDRESS

Rahaf Issa, Division of Pharmacy and Optometry, University of Manchester, Manchester, United Kingdom

Fawzyah Albaldi, Department of Biology, Al-Baha University, Alaqiq, Saudi Arabia

Lucy Urwin, School of Biosciences, University of Sheffield, Sheffield, United Kingdom

AUTHOR ORCIDs

Luke R. Green http://orcid.org/0000-0002-2836-2041

Claire E. Turner http://orcid.org/0000-0002-4458-9748

FUNDING

AUTHOR CONTRIBUTIONS

Luke R. Green, Conceptualization, Formal analysis, Funding acquisition, Investigation, Methodology, Visualization, Writing – original draft, Writing – review and editing | Rahaf Issa, Methodology, Writing – review and editing | Fawzyah Albaldi, Investigation, Methodology, Writing – review and editing | Lucy Urwin, Investigation, Writing – review and editing | Ruth Thompson, Investigation, Methodology, Writing – review and editing | Henna Khalid, Methodology, Writing – review and editing | Claire E. Turner, Methodology, Writing – review and editing | Barbara Ciani, Conceptualization, Writing – review and editing | Lynda J. Partridge, Conceptualization, Funding acquisition, Methodology,

Writing – review and editing, Supervision | Peter N. Monk, Conceptualization, Funding acquisition, Investigation, Methodology, Writing – original draft, Writing – review and editing, Supervision

ADDITIONAL FILES

The following material is available online.

Supplemental Material

Fig. S1 (mBio01482-23-S0001.tif). Knockout or knockdown of CD9 and putative staphylococcal receptors reduces *S. aureus* adhesion to A549 cells.

Fig. S2 (mBio01482-23-S0002.tif). CD9-derived peptides and unfractionated heparin do not affect staphylococcal growth at concentrations which reduce staphylococcal adherence.

Fig. S3 (mBio01482-23-S0003.tif). CD9-derived peptides, heparin analogues and removal of heparan sulfates reduce staphylococcal adherence in Tspan15$^{-/-}$ cells.

Fig. S4 (mBio01482-23-S0004.tif). 800C interacts with cells expressing CD9 and specifically inhibits staphylococcal adherence.

Fig. S5 (mBio01482-23-S0005.tif). CD9-derived peptides can affect clinical *S. aureus* isolates and reduce staphylococcal adhesion to human keratinocytes similar to heparin analogue treatments.

Fig. S6 (mBio01482-23-S0006.tif). Various anti-α5β1 antibodies have little effect on staphylococcal adherence to human keratinocytes.

Fig. S7 (mBio01482-23-S0007.tif). Reduction of staphylococcal adhesion using either CD9-derived peptides or unfractionated heparin in various cell lines.

Fig. S8 (mBio01482-23-S0008.tif). Confirmation of SDC knockdown in A549 cells with shRNA.

Fig. S9 (mBio01482-23-S0009.tif). Fn bacterial binding increases after treatment with exogenous Fn but does not increase binding of a Δ*fnb* mutant.

REFERENCES

1. Tong SYC, Davis JS, Eichenberger E, Holland TL, Fowler VG. 2015. *Staphylococcus aureus* infections: epidemiology, pathophysiology, clinical manifestations, and management. Clin Microbiol Rev 28:603–661. https://doi.org/10.1128/CMR.00134-14

2. Stryjewski ME, Corey GR. 2014. Methicillin-resistant *Staphylococcus aureus*: an evolving pathogen. Clin Infect Dis 58:S10–9. https://doi.org/10.1093/cid/cit613

3. Josse J, Laurent F, Diot A. 2017. Staphylococcal adhesion and host cell invasion: fibronectin-binding and other mechanisms. Front Microbiol 8:2433. https://doi.org/10.3389/fmicb.2017.02433

4. Sinha B, François PP, Nüsse O, Foti M, Hartford OM, Vaudaux P, Foster TJ, Lew DP, Herrmann M, Krause KH. 1999. Fibronectin-binding protein acts as *Staphylococcus aureus* invasin via fibronectin bridging to integrin α5β1. Cell Microbiol 1:101–117. https://doi.org/10.1046/j.1462-5822.1999.00011.x

5. Hess DJ, Henry-Stanley MJ, Erlandsen SL, Wells CL. 2006. Heparan sulfate proteoglycans mediate *Staphylococcus aureus* interactions with intestinal epithelium. Med Microbiol Immunol 195:133–141. https://doi.org/10.1007/s00430-005-0007-5

6. Chen Y, Götte M, Liu J, Park PW. 2008. Microbial subversion of heparan sulfate proteoglycans. Mol Cells 26:415–426.

7. Rajas O, Quirós LM, Ortega M, Vazquez-Espinosa E, Merayo-Lloves J, Vazquez F, García B. 2017. Glycosaminoglycans are involved in bacterial adherence to lung cells. BMC Infect Dis 17:319. https://doi.org/10.1186/s12879-017-2418-5

8. García B, Merayo-Lloves J, Rodríguez D, Alcalde I, García-Suárez O, Alfonso JF, Baamonde B, Fernández-Vega A, Vazquez F, Quirós LM. 2016. Different use of cell surface Glycosaminoglycans as adherence receptors to corneal cells by gram positive and gram negative pathogens. Front Cell Infect Microbiol 6:173. https://doi.org/10.3389/fcimb.2016.00173

9. Hayashida A, Amano S, Park PW. 2011. Syndecan-1 promotes *Staphylococcus aureus* corneal infection by counteracting neutrophil-mediated host defense. J Biol Chem 286:3288–3297. https://doi.org/10.1074/jbc.M110.185165

10. Gong W, Liu Y, Huang B, Lei Z, Wu F-H, Li D, Feng Z-H, Zhang G-M. 2008. Recombinant CBD-HepII polypeptide of fibronectin inhibits αvβ3 signaling and hematogenous metastasis of tumor. Biochem Biophys Res Commun 367:144–149. https://doi.org/10.1016/j.bbrc.2007.12.110

11. Yang N, Friedl A. 2016. Syndecan-1-induced ECM fiber alignment requires integrin αvβ3 and syndecan-1 ectodomain and heparan sulfate chains. PLoS One 11:e0150132. https://doi.org/10.1371/journal.pone.0150132

12. Jinno A, Hayashida A, Jenkinson HF, Park PW. 2020. Syndecan-1 promotes Streptococcus pneumoniae corneal infection by facilitating the assembly of adhesive fibronectin fibrils. mBio 11:e01907-20. https://doi.org/10.1128/mBio.01907-20

13. Hemler ME. 2005. Tetraspanin functions and associated microdomains. Nat Rev Mol Cell Biol 6:801–811. https://doi.org/10.1038/nrm1736

14. Umeda R, Satouh Y, Takemoto M, Nakada-Nakura Y, Liu K, Yokoyama T, Shirouzu M, Iwata S, Nomura N, Sato K, Ikawa M, Nishizawa T, Nureki O. 2020. Structural insights into tetraspanin CD9 function. Nat Commun 11:1606. https://doi.org/10.1038/s41467-020-15459-7

15. Zimmerman B, Kelly B, McMillan BJ, Seegar TCM, Dror RO, Kruse AC, Blacklow SC. 2016. Crystal structure of a full-length human tetraspanin reveals a cholesterol-binding pocket. Cell 167:1041–1051. https://doi.org/10.1016/j.cell.2016.09.056

16. Yang Y, Liu XR, Greenberg ZJ, Zhou F, He P, Fan L, Liu S, Shen G, Egawa T, Gross ML, Schuettpelz LG, Li W. 2020. Open conformation of tetraspanins shapes interaction partner networks on cell membranes. EMBO J 39:e105246. https://doi.org/10.15252/embj.2020105246

17. Barreiro O, Zamai M, Yáñez-Mó M, Tejera E, López-Romero P, Monk PN, Gratton E, Caiolfa VR, Sánchez-Madrid F. 2008. Endothelial adhesion receptors are recruited to adherent leukocytes by inclusion in preformed tetraspanin nanoplatforms. J Cell Biol 183:527–542. https://doi.org/10.1083/jcb.200805076

18. Karam J, Méresse S, Kremer L, Daher W. 2020. The roles of tetraspanins in bacterial infections. Cell Microbiol 22:e13260. https://doi.org/10.1111/cmi.13260

19. Florin L, Lang T. 2018. Tetraspanin assemblies in virus infection. Front Immunol 9:1140. https://doi.org/10.3389/fimmu.2018.01140

20. Green LR, Monk PN, Partridge LJ, Morris P, Gorringe AR, Read RC. 2011. Cooperative role for tetraspanins in adhesin-mediated attachment of bacterial species to human epithelial cells. Infect Immun 79:2241–2249. https://doi.org/10.1128/IAI.01354-10

21. Ventress JK, Partridge LJ, Read RC, Cozens D, MacNeil S, Monk PN. 2016. Peptides from tetraspanin CD9 are potent inhibitors of *Staphylococcus aureus* adherence to keratinocytes. PLoS One 11:e0160387. https://doi.org/10.1371/journal.pone.0160387

22. Zhou G, Mo WJ, Sebbel P, Min G, Neubert TA, Glockshuber R, Wu XR, Sun TT, Kong XP. 2001. Uroplakin Ia is the urothelial receptor for uropathogenic *Escherichia coli*: evidence from *in vitro* FimH binding. J Cell Sci 114:4095–4103. https://doi.org/10.1242/jcs.114.22.4095

23. Karam J, Blanchet FP, Vivès É, Boisguérin P, Boudehen Y-M, Kremer L, Daher W. 2023. *Mycobacterium Abscessus* A\alkyl hydroperoxide reductase C promotes cell invasion by binding to tetraspanin CD81. iScience 26:106042. https://doi.org/10.1016/j.isci.2023.106042

24. Blake DJ, Martiszus JD, Lone TH, Fenster SD. 2018. Ablation of the CD9 receptor in human lung cancer cells using CRISPR/Cas alters migration to chemoattractants including IL-16. Cytokine 111:567–570. https://doi.org/10.1016/j.cyto.2018.05.038

25. Grayson AK, Hearnden V, Bolt R, Jebreel A, Colley HE, Murdoch C. 2018. Use of a Rho kinase inhibitor to increase human tonsil keratinocyte longevity for three-dimensional, tissue engineered tonsil epithelium equivalents. J Tissue Eng Regen Med 12:e1636–e1646. https://doi.org/10.1002/term.2590

26. Pasqualon T, Pruessmeyer J, Weidenfeld S, Babendreyer A, Groth E, Schumacher J, Schwarz N, Denecke B, Jahr H, Zimmermann P, Dreymueller D, Ludwig A. 2015. A transmembrane C-terminal fragment of syndecan-1 is generated by the metalloproteinase ADAM17 and promotes lung epithelial tumor cell migration and lung metastasis formation. Cell Mol Life Sci 72:3783–3801. https://doi.org/10.1007/s00018-015-1912-4

27. Pasqualon T. 2015. Thesis. *In vivo* and *in vitro* analysis of syndecan-1 and syndecan-4 cleavage fragments as regulators of cell migration. Available from: http://publications.rwth-aachen.de/record/561336/files/561336.pdf

28. Lipper CH, Gabriel K-H, Seegar TCM, Dürr KL, Tomlinson MG, Blacklow SC. 2022. Crystal structure of the Tspan15 LEL domain reveals a conserved ADAM10 binding site. Structure 30:206–214. https://doi.org/10.1016/j.str.2021.10.007

29. Aquino RS, Park PW. 2016. Glycosaminoglycans and infection. Front Biosci (Landmark Ed) 21:1260–1277. https://doi.org/10.2741/4455

30. Jaffer IH, Weitz JI. 2018. Antithrombotic drugs, p 2168–2188. In Silberstein LE, J Anastasi, R Hoffman, EJ Benz, H Heslop, J Weitz (ed), Hematology: Basic principles and practice, 7th ed. Elsevier Inc.

31. Bauer KA, Hawkins DW, Peters PC, Petitou M, Herbert J-M, van Boeckel CAA, Meuleman DG. 2002. Fondaparinux, a synthetic pentasaccharide: the first in a new class of antithrombotic agents - the selective factor Xa inhibitors. Cardiovasc Drug Rev 20:37–52. https://doi.org/10.1111/j.1527-3466.2002.tb00081.x

32. Dredge K, Brennan TV, Hammond E, Lickliter JD, Lin L, Bampton D, Handley P, Lankesheer F, Morrish G, Yang Y, Brown MP, Millward M. 2018. A phase I study of the novel immunomodulatory agent PG545 (Pixatimod) in subjects with advanced solid tumours. Br J Cancer 118:1035–1041. https://doi.org/10.1038/s41416-018-0006-0

33. Jones PH, Bishop LA, Watt FM. 1996. Functional significance of CD9 association with β1 integrins in human epidermal keratinocytes. Cell Adhes Commun 4:297–305. https://doi.org/10.3109/15419069609010773

34. Kim CW, Goldberger OA, Gallo RL, Bernfield M. 1994. Members of the yndecan family of heparan sulfate proteoglycans are expressed in distinct cell-, tissue-, and development-specific patterns. Mol Biol Cell 5:797–805. https://doi.org/10.1091/mbc.5.7.797

35. Mould AP, Askari JA, Byron A, Takada Y, Jowitt TA, Humphries MJ. 2016. Ligand-induced EPITOPE masking: dissociation of integrin A5B1-fibronectin complexes only by monoclonal antibodies with an allosteric mode of action. J Biol Chem 291:20993–21007. https://doi.org/10.1074/jbc.M116.736942

36. Machado-Pineda Y, Cardeñes B, Reyes R, López-Martín S, Toribio V, Sánchez-Organero P, Suarez H, Grötzinger J, Lorenzen I, Yáñez-Mó M, Cabañas C. 2018. CD9 controls integrin α5β1-mediated cell adhesion by modulating its association with the metalloproteinase ADAM17. Front Immunol 9:2474. https://doi.org/10.3389/fimmu.2018.02474

37. Stepp MA, Daley WP, Bernstein AM, Pal-Ghosh S, Tadvalkar G, Shashurin A, Palsen S, Jurjus RA, Larsen M. 2010. Syndecan-1 regulates cell migration and fibronectin fibril assembly. Exp Cell Res 316:2322–2339. https://doi.org/10.1016/j.yexcr.2010.05.020

38. Galante LL, Schwarzbauer JE. 2007. Requirements for sulfate transport and the diastrophic dysplasia sulfate transporter in fibronectin matrix assembly. J Cell Biol 179:999–1009. https://doi.org/10.1083/jcb.200707150

39. Arciola CR, Bustanji Y, Conti M, Campoccia D, Baldassarri L, Samorì B, Montanaro L. 2003. *Staphylococcus* Epidermidis-fibronectin binding and its inhibition by heparin. Biomaterials 24:3013–3019. https://doi.org/10.1016/s0142-9612(03)00133-9

40. Hayashida A, Amano S, Gallo RL, Linhardt RJ, Liu J, Park PW. 2015. 2-O-sulfated domains in Syndecan-1 heparan sulfate inhibit neutrophil cathelicidin and promote *Staphylococcus aureus* corneal infection. J Biol Chem 290:16157–16167. https://doi.org/10.1074/jbc.M115.660852

41. Park PW, Pier GB, Hinkes MT, Bernfield M. 2001. Exploitation of Syndecan-1 shedding by *Pseudomonas aeruginosa* enhances virulence. Nature 411:98–102. https://doi.org/10.1038/35075100

42. Speziale P, Arciola CR, Pietrocola G. 2019. Fibronectin and its role in human infective diseases. Cells 8:1516. https://doi.org/10.3390/cells8121516

43. Mayor S, Riezman H. 2004. Sorting GPI-anchored proteins. Nat Rev Mol Cell Biol 5:110–120. https://doi.org/10.1038/nrm1309

44. Grigorov B, Reungoat E, Gentil Dit Maurin A, Varbanov M, Blaising J, Michelet M, Manuel R, Parent R, Bartosch B, Zoulim F, Ruggiero F, Pécheur E-I. 2017. Hepatitis C virus infection propagates through interactions between Syndecan-1 and CD81 and impacts the hepatocyte glycocalyx. Cell Microbiol 19. https://doi.org/10.1111/cmi.12711

45. Couchman JR. 2010. Transmembrane signaling proteoglycans. Annu Rev Cell Dev Biol 26:89–114. https://doi.org/10.1146/annurev-cellbio-100109-104126

46. Araki E, Momota Y, Togo T, Tanioka M, Hozumi K, Nomizu M, Miyachi Y, Utani A. 2009. Clustering of Syndecan-4 and integrin β1 by laminin α3 chain-derived peptide promotes keratinocyte migration. Mol Biol Cell 20:3012–3024. https://doi.org/10.1091/mbc.e08-09-0977

47. Morgan MR, Humphries MJ, Bass MD. 2007. Synergistic control of cell adhesion by integrins and Syndecans. Nat Rev Mol Cell Biol 8:957–969. https://doi.org/10.1038/nrm2289

48. Cook GA, Wilkinson DA, Crossno JT, Raghow R, Jennings LK. 1999. The tetraspanin Cd9 influences the adhesion, spreading, and Pericellular fibronectin matrix assembly of Chinese Hamster ovary cells on human plasma fibronectin. Exp Cell Res 251:356–371. https://doi.org/10.1006/excr.1999.4596

49. Kotha J, Longhurst C, Appling W, Jennings LK. 2008. Tetraspanin CD9 regulates β1 integrin activation and enhances cell motility to fibronectin via a PI-3 kinase-dependent pathway. Exp Cell Res 314:1811–1822. https://doi.org/10.1016/j.yexcr.2008.01.024

50. Cook GA, Longhurst CM, Grgurevich S, Cholera S, Crossno JT, Jennings LK. 2002. Identification of CD9 extracellular domains important in regulation of CHO cell adhesion to fibronectin and fibronectin pericellular matrix assembly. Blood 100:4502–4511. https://doi.org/10.1182/blood.V100.13.4502

51. Liang X, Garcia BL, Visai L, Prabhakaran S, Meenan NAG, Potts JR, Humphries MJ, Höök M, Bouvard D. 2016. Allosteric regulation of fibronectin/α5β1 interaction by fibronectin-binding MSCRAMMs. PLoS ONE 11:e0159118. https://doi.org/10.1371/journal.pone.0159118

52. Niemann S, Nguyen MT, Eble JA, Chasan AI, Mrakovcic M, Böttcher RT, Preissner KT, Roßlenbroich S, Peters G, Herrmann M. 2021. More is not

always better—the double-headed role of fibronectin in *Staphylococcus aureus* host cell invasion. mBio 12:e0106221. https://doi.org/10.1128/mBio.01062-21

53. Lyon LM, Doran KS, Horswill AR. 2023. *Staphylococcus aureus* fibronectin-binding proteins contribute to colonization of the female reproductive tract. Infect Immun 91:e0046022. https://doi.org/10.1128/iai.00460-22

54. Monk PN, Issa R, Ciani B. 2021. Antimicrobial target. WO. 2021/175809 A1. World Intellectual Property Organization, GB.

55. Shanks RMQ, Donegan NP, Graber ML, Buckingham SE, Zegans ME, Cheung AL, O'Toole GA. 2005. Heparin stimulates *Staphylococcus aureus* biofilm formation. Infect Immun 73:4596–4606. https://doi.org/10.1128/IAI.73.8.4596-4606.2005

56. Hammond E, Dredge K. 2020. Heparanase inhibition by Pixatimod (PG545): basic aspects and future perspectives. Adv Exp Med Biol 1221:539–565. https://doi.org/10.1007/978-3-030-34521-1_22

57. Guimond SE, Mycroft-West CJ, Gandhi NS, Tree JA, Le TT, Spalluto CM, Humbert MV, Buttigieg KR, Coombes N, Elmore MJ, Wand M, Nyström K, Said J, Setoh YX, Amarilla AA, Modhiran N, Sng JDJ, Chhabra M, Young PR, Rawle DJ, Lima MA, Yates EA, Karlsson R, Miller RL, Chen Y-H, Bagdonaite I, Yang Z, Stewart J, Nguyen D, Laidlaw S, Hammond E, Dredge K, Wilkinson TMA, Watterson D, Khromykh AA, Suhrbier A,

Carroll MW, Trybala E, Bergström T, Ferro V, Skidmore MA, Turnbull JE. 2022. Synthetic Heparan sulfate mimetic Pixatimod (PG545) potently inhibits SARS-CoV-2 by disrupting the spike–ACE2 interaction. ACS Cent Sci 8:527–545. https://doi.org/10.1021/acscentsci.1c01293

58. Lundin A, Bergström T, Andrighetti-Fröhner CR, Bendrioua L, Ferro V, Trybala E. 2012. Potent anti-respiratory syncytial virus activity of a cholestanol-sulfated tetrasaccharide conjugate. Antiviral Res 93:101–109. https://doi.org/10.1016/j.antiviral.2011.11.002

59. Modhiran N, Gandhi NS, Wimmer N, Cheung S, Stacey K, Young PR, Ferro V, Watterson D. 2019. Dual targeting of Dengue virus Virions and Ns1 protein with the Heparan sulfate mimic PG545. Antiviral Res 168:121–127. https://doi.org/10.1016/j.antiviral.2019.05.004

60. Said J, Trybala E, Andersson E, Johnstone K, Liu L, Wimmer N, Ferro V, Bergström T. 2010. Lipophile-conjugated sulfated oligosaccharides as novel microbicides against HIV-1. Antiviral Research 86:286–295. https://doi.org/10.1016/j.antiviral.2010.03.011

61. Said JS, Trybala E, Görander S, Ekblad M, Liljeqvist J-Å, Jennische E, Lange S, Bergström T. 2016. The cholestanol-conjugated sulfated oligosaccharide PG545 disrupts the lipid envelope of herpes simplex virus particles. Antimicrob Agents Chemother 60:1049–1057. https://doi.org/10.1128/AAC.02132-15